

Content from this work may be used under the terms of the CC BY 3.0 licence (© 2016). Any distribution of this work must maintain attribution to the author(s), title of the work, publisher, and DOI.

# THERMAL MANAGEMENT AND CRYSTAL CLAMPING CONCEPTS FOR THE NEW HIGH-DYNAMICS DCM FOR SIRIUS

M. Saveri Silva\*, R. R. Geraldés, A. Gilmour, LNLs, Campinas, Brazil  
 T. A. M. Ruijl, R. M. Schneider, MI Partners, Eindhoven, Netherlands

## Abstract

The monochromator is known to be one of the most critical optical elements of a synchrotron beamline, since it directly affects the beam quality with respect to energy and position. Naturally, the new 4th generation machines, with emittances in the range of order of 100 pm rad, require even higher stability performances, in spite of the still conflicting factors such as high power loads, power load variation, and vibration sources. A new high-dynamics DCM (Double Crystal Monochromator) is under development at the Brazilian Synchrotron Light Laboratory for the future X-ray undulator and superbend beamlines of Sirius, the new Brazilian 4th generation synchrotron [1, 2]. In order to achieve high-bandwidth control and stability of a few nrad, as well as to prevent unpredicted mounting and clamping distortions, new solutions are proposed for crystal fixation and thermal management. The design is based on flexural elements, aiming for a highly predictable performance, like support stiffness, crystal distortion and thermal insulation. It was optimised by using mechanical and thermal FEA, including CFD. Efforts were made to predict thermal boundaries associated with the synchrotron beam, including incident, diffracted and scattered power, for which the undulator spectrum was employed in the Monte Carlo simulation package – FLUKA.

## INTRODUCTION

The goal of this work is to present the thermal management and the mechanical clamping concepts for the new high stability DCM for Sirius. Details about the full system and its specifications can be found in [3].

## THERMAL MANAGEMENT

The first step towards modelling the thermal behaviour of the system was collecting power loads and boundary conditions.

### Incident Power

Taking 19 mm period undulator as the source (with 105 periods and at 350 mA current), its spectrum was simulated using SPECTRA [4] and post-processed in MATLAB [5] in order to find both the total incident power and the power variation for energy scans as a function of energy. The results are presented in Fig. 1 and it can be seen that the power load does not exceed 150 W. However, the DCM has to deal with a variation of more than 100 W over the full range, and as much as 38 W for 1 keV scans.

From the total incident power, most of it is absorbed by the 1st crystal (CRYS1), whereas a small fraction of it is

diffracted and the remaining of it is scattered. These quantities have been estimated for a better comprehension of each contribution to the system.

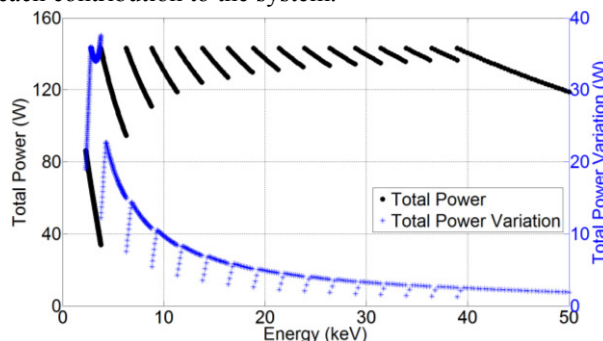


Figure 1: Incident power and power variation in  $\pm 0.5$  keV scans as a function of energy for Si (111) with an acceptance of  $60 \times 60 \mu rad^2$ .

### Absorption and Scattering

A user routine was implemented into the Monte Carlo package FLUKA [6, 7] in order to guide the design of the shielding structure, to estimate the radiation doses in sensitive elements and to evaluate the deposited energy in the main components after scattering and absorption. Both the Bremsstrahlung flux, generated inside FLUKA from the electron beam, and the synchrotron flux, imported from SRW [8], have been evaluated. The first was found to be several orders of magnitude smaller than latter, so that its contribution could be neglected regarding power levels. Super MC [9, 10] was used to convert CAD drawings in FLUKA geometries. Figure 2 shows the original simplified CAD model and its conversion inside FLUKA, as well as some results of the photon track length density for different shielding designs.

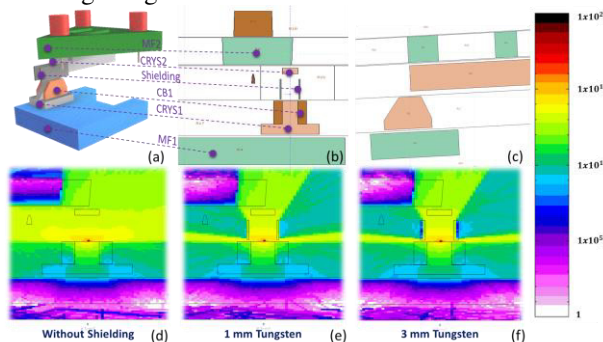


Figure 2: FLUKA simulations: (a) original CAD model; (b) upstream view of the model in FLUKA; (c) side view of the model in FLUKA; (d) to (f) upstream view of photon track length density (Particles/cm<sup>2</sup>/s) for three shielding designs.

\* marlon.saveri@lnls.br

As expected, the simulations have shown that the scattering profiles strongly depend on photon energy and incidence angle. Therefore, the power distribution over the components also strongly depends on the Bragg angle ( $\theta$ ) and  $K$ -value of the undulator. Table 1 resumes the percentage of power that is absorbed by the 1<sup>st</sup> and 2<sup>nd</sup> crystals (CRYS1 and CRY2, respectively) with respect to the incident power in four representative scenarios.

Table 1: Power Absorption in Crystals

Scenario	CRYS1 (%)	CRYS2 (%)
3°, K=2.27	95.54	1.02
3°, K=0.62	99.00	0.07
60°, K=2.27	98.38	0.15
60°, K=0.62	99.57	0.02

### Diffraction Power

The diffracted power was estimated by applying the energy selection of each crystal to the flux spectra weighted by the photon energy. The highest levels of diffracted power occur for low energies and with the Si (111) crystal, when compared to Si(311). This is not only because at low energies the flux is higher and the Darwin Width (DW) of both crystals is larger, but also because the DW of Si(111) is larger than that of Si(311). As expected, the magnitude of the diffracted beam is very small when compared to the incident one, but it is already in the same order of magnitude of scattered power, reaching 0.7 W. Fortunately, most of this power should also be diffracted by CRY2 and leave the DCM.

### Black Body Radiation

Since a few key elements in the crystal cage work at low temperatures, the irradiation power contribution has also been investigated. A simple model was built in ANSYS [11] with roughly similar geometry to that of the crystal cage of the DCM. The main interest was the evaluation for CRY1 and CRY2, and their metrology frames, MF1 and MF2. As an approximation, a general emissivity of 0.1 has been considered. Table 2 shows the designed temperature target and the resulting power absorption for each element. Since the resulting numbers are non-negligible, they have become part of the thermal management strategy.

Table 2: Black Body Radiation FEA Estimate

Element	Temperature (K)	FEA Result (W)
CRYS1	80	0.4
MF1	150	3.8
CRYS2	155	0.9
MF2	213	2.7

### Thermal Model

In order to define a consistent thermal management strategy, a lumped-mass thermal model has been developed for the DCM core, as depicted in Fig. 3. In order to control the temperature of the second crystal and prevent cooling

down of surrounding parts, several local heaters with temperature sensors are applied, so that the temperature at YFM, SSF and CRY2 are controlled at 22°C, 22°C and 155 K, respectively. The approximated heat input by the local heaters is also depicted in the figure (arrows). Finally, each link between two nodes defines the thermal conductance ( $g_i$ ) between them, as seen in Table 3. The conductance values were evaluated by hand calculation and FEA, also taking into account references from literature [12].

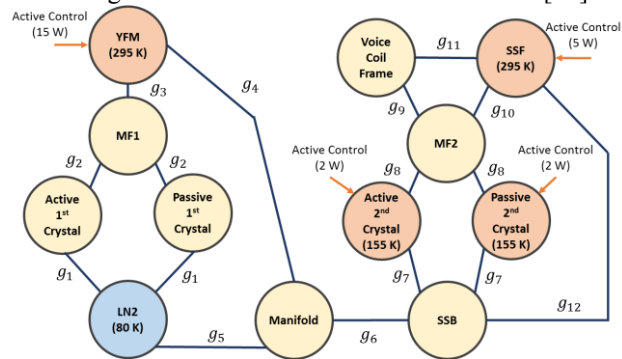


Figure 3 – Thermal Model.

Table 3: Thermal Conductances

Link	Description	$g$ (W/K)
g1	LN2 HTC (block) + Cu + In + Si	36
g2	CRYS1 mount on MF1	0.081
g3	MF1 mount on YFM	0.057
g4	Manifold mount on YFM	0.025
g5	LN2 HTC (manifold)	10
g6	High-conductivity copper strap	0.750
g7	CRYS2 compliant copper strap	0.100
g8	CRYS2 mount on MF2	0.055
g9	Voice Coil mount on MF2	0.048
g10	Leaf springs	0.018
g11	Voice Coil copper straps	0.030
g12	SSB mount on SSF	0.020

No water cooling is considered in this project in order to prevent the need of a thermal bath and more sophisticated cooling design, as vacuum guards, for instance. Instead, most of the power load is taken by the LN<sub>2</sub> system, whereas the chamber and the environment work as an auxiliary heat sink.

### Cooling Design

CRYS1 will be indirectly cryogenically cooled by copper blocks (CB1), which are clamped at both sides of the crystal via three fasteners and disc washers, to guarantee the clamping pressure over thermal expansion. The fastener that is close to the diffraction plane should deliver 50 N, whereas the two others are allowed to be stronger, with 125 N each. Each cooling block is a brazed structure made of three separate parts, creating two circular channels, through which LN<sub>2</sub> flows in opposite directions in order to better balance disturbances. Ideally, a laminar flow should be chosen for minimum vibration levels, however,

Content from this work may be used under the terms of the CC BY 3.0 licence (© 2016). Any distribution of this work must maintain attribution to the author(s), title of the work, publisher, and DOI.

this condition was insufficient to keep the hotspot temperature below 130 K, as specified. Thus, turbulent flow ( $Re \approx 40000$ ) was chosen to achieve a higher heat transfer coefficient (HTC). Analytical estimates and CFD were used to simulate the performance of several cooling layouts, aiming for high HTC and minimum velocity change, which is considered to be correlated with vibrations levels [13]. The best solution found so far is outlined in Fig. 4, but 3D-printed options are also under evaluation. The small internal diameter, only 2 mm, matches that of the low-stiffness pipes and allows for an increased effective contact area between the fluid and the block.

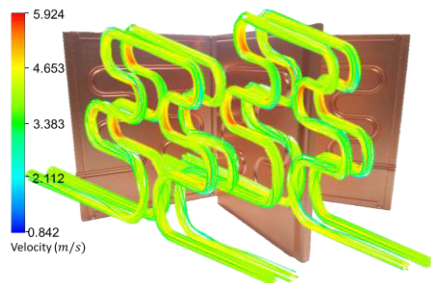


Figure 4 - Cooling channels prototype and velocity distribution obtained by CFD analysis.

An indium layer is used for increasing the heat exchange between CRY1 and CB1, as well as the deformation of CRY1 due to clamping and thermal expansion effects. Indeed, the difference in thermal expansion in the cooling processes from room temperature to cryogenic temperatures may cause non-negligible stresses and strains. As for CRY2, it will be cooled by copper straps (HCS and CCS) linked to an extension of the manifold (CMX), as displayed in Fig. 5.

### CLAMPING CONCEPTS

Strict stability performance and positioning tolerances for metrology require not only well designed structures, but also adequate contact interface and coupling between elements, so that high stiffness and high eigenfrequencies can be achieved. Nevertheless, as already mentioned, different thermal expansions might result in unacceptable stresses and deformations, not only in the crystals but also in the metrology frames. Furthermore, the thermal model requires low thermal conductance of some of these connections in order to limit active heating power and manage thermal sensitivity. Thus, there should be an appropriate compromise between stiffness and thermal conductance in fixing the crystals and metrology frames.

Kinematic mounts (as spheres in V-grooves) have been considered for crystal mounting. However, the static friction stiffness is something difficult to be precisely predicted, so that it might lead to uncertain accommodation of the thermal expansion and deformations. Thus, this solution was replaced by fixing each crystal on three wire-eroded flexures in MF1 and MF2 (inset in Fig. 5), which can be more deterministically designed. An optimization process was applied to design them in order to minimize the thermal conductivity, while maximizing stiffness in the

principle supporting degrees of freedom and minimizing it in the principle compliant degrees of freedom, so that the crystals may relatively freely expand. Table 4 shows FEA results for CRY2 assembly on MF2, including stresses and deformation (slope error) due to the cooling down process.

Table 4: Results Using Flexures for CRY2 Clamping

Property	Value
1 <sup>st</sup> Eigen Frequency	1.7 kHz
Stiffness in stiff direction (x3)	$1 \times 10^8 \text{ Nm}^{-1}$
Stiffness in compliant direction	$1 \times 10^5 \text{ Nm}^{-1}$
Maximum principal stress in CRY2	1.4 MPa
Slope error on footprint ( $\theta=3^\circ$ )	0.19 $\mu\text{rad}$

The preload applied in each fastener has to be high enough to overcome the resulting forces from actuators, gravity effects, disturbances and assembly misalignments, but must not cause large deformations on the diffraction plane nor exceed the stress limits in the crystals. Taking these effects into account and considering that the fastening system should as well guarantee the clamping forces over thermal expansion, a suitable composition of disc washers is used to deliver 320 N per fastener.

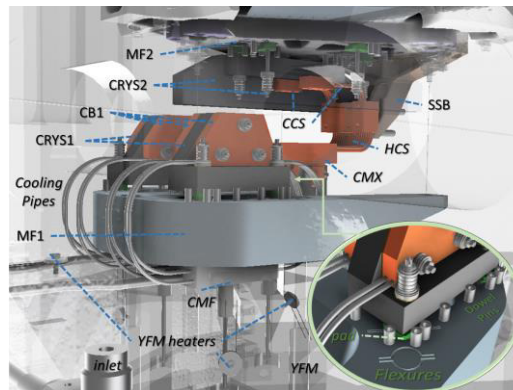


Figure 5 – Main elements related to the solutions proposed for cooling and clamping of crystals.

### CONCLUSION

This work briefly described the thermal and clamping solutions for the new high-dynamics DCM for Sirius, which are important to guarantee the integrity and optimum performance of the crystals. Several analytical and numerical tools have been used in order to design them with specific targets regarding slope errors, thermal response, mechanical stiffness and manufacturability. This work will continue during the Detailed Design Phase and, after validation, may be extended to different systems, such as mirrors and other monochromators.

### ACKNOWLEDGEMENT

The authors would like to gratefully acknowledge the funding by the Brazilian Ministry of Science, Technology, Innovation and Communication and the contributions of the LNLS team, notably Materials and Optics groups, and the MI-Partners team.



## REFERENCES

- [1] L. Liu, F. H. de Sá, and X. R. Resende, "A new optics for Sirius," in *Proc. IPAC'2016*, pp. 3413–3415.
- [2] A. Rodrigues *et al.*, "Sirius Status Report", in *Proc. IPAC'16*, Busan, Korea, May 2016, paper WEPOW001, pp. 2811-2814.
- [3] R. Geraldès *et al.*, "The new high dynamics DCM for Sirius", presented at MEDSI 2016, Barcelona, Spain, Sep. 2016, this conference.
- [4] T. Tanaka and H. Kitamura, "Spectra: a synchrotron radiation calculation code", *Journal of Synchrotron Radiation*, vol. 8, pp. 1221-1228, Nov. 2001.
- [5] MATLAB Release 2011b, The MathWorks, Inc., Natick, MA, USA.
- [6] T. Böhlen *et al.*, "The FLUKA code: developments and challenges for high energy and medical applications". *Nuclear Data Sheets*, vol. 120, pp. 211-214, 2014.
- [7] A. Ferrari *et al.*, "FLUKA: a multi-particle transport code". CERN-2005-10, INFN/TC\_05/11, SLAC-R-773, 2005.
- [8] O. Chubar, P. Elleaume, "Accurate and efficient computation of synchrotron radiation in the near field region", in *Proc. of the EPAC98 Conference*, Jun 1998, pp. 1177-1179.
- [9] Y. Wu, "CAD-based interface programs for fusion neutron transport simulation", *Fusion Engineering and Design*, vol. 84, pp. 1987-1992, Feb. 2009.
- [10] Y. Wu, J. Song, H. Zheng *et al.*, "CAD-Based Monte Carlo program for integrated simulation of nuclear system Super MC", *Ann. Nucl.*, vol. 82 pp. 161-168, Aug. 2015.
- [11] ANSYS® Academic Research, Release 17.1.
- [12] P. Marion, L. Zhang, L. Goirand, M. Rossat, and K. Martel, "Cryogenic cooling of monochromator crystals: indirect or direct cooling?" in *Proc. MEDSI 2006*, Hyogo, Japan, May 2006.
- [13] R. Caliarì *et al.*, "Studies on flow-induced-vibrations for the new high-dynamics DCM for Sirius", presented at MEDSI 2016, Barcelona, Spain, Sep. 2016, this conference.